

UNIVERSIDADE DE SÃO PAULO

# PUBLICAÇÕES

INSTITUTO DE FÍSICA  
CAIXA POSTAL 20516  
01498 - SÃO PAULO - SP  
BRASIL

IFUSP/P-532

ELASTIC ENHANCEMENT FACTOR IN THE  $^{11}\text{B}(p,n_0)^{11}\text{C}$   
REACTION AT  $E_p = 14.3$  MeV

by

M.S. Hussein and E. Farrelly Pessoa

Instituto de Física, Universidade de São Paulo  
and

H.R. Schelin and B.V. Carlson

Divisão de Física Teórica, Instituto de Estudos  
Avançados, Centro Técnico Aeroespacial, C.P. 6044,  
12200 São José dos Campos, S.P., Brasil

and

R.A. Douglas

IFGW, Universidade de Campinas,  
13100 Campinas, S.P., Brasil

Maio/1985

ELASTIC ENHANCEMENT FACTOR IN THE  $^{11}\text{B}(p,n_0)^{11}\text{C}$

REACTION AT  $E_p = 14.3$  MeV

M.S. Hussein and E. Farrelly Pessoa

Instituto de Física, Departamento de Física Nuclear,  
Universidade de São Paulo, C.P. 20.516, 01498 São Paulo,  
S.P., Brasil

and

H.R. Schelin and B.V. Carlson

Divisão de Física Teórica, Instituto de Estudos Avançados,  
Centro Técnico Aeroespacial, C.P. 6044,  
12200 São José dos Campos, S.P., Brasil

and

R.A. Douglas

IFGW, Universidade de Campinas,  
13100 Campinas, S.P., Brasil

ABSTRACT

The elastic enhancement factor in charge exchange reactions proceeding via the compound nucleus, predicted to attain the value of 2 in the weak isospin mixing regime by Harney, Weidenmüller and Richter five years ago, is tested here in the system  $^{11}\text{B}(p,n)^{11}\text{C}$  at  $\langle E_p \rangle = 14.3$  MeV. Both the DWBA and Hauser-Feshbach calculations employed in the analysis are used in a way which physically simulates a two coupled-channels model. Our results show an enhancement factor larger than 1 indicating that isospin is mainly conserved in this reaction.

The elastic enhancement factor in statistical nuclear reactions (those that proceed via the compound nucleus), which is predicted to be about 2 in the strong absorption limit<sup>1,2)</sup>, is an important deviation from the simple Hauser-Feshbach description. Back in 1978, Kretschmer and Wangler<sup>3)</sup> gave a very nice and convincing experimental verification of the existence of this factor in the compound elastic process  $^{28}\text{Si}(p,p)^{28}\text{Si}$  at  $E_p = 9.8$  MeV. Subsequently, Harney, Weidenmüller and Richter<sup>4)</sup> (HWR) suggested that charge exchange reactions proceeding through the compound nucleus should also show the above feature of compound elastic scattering namely, they are enhanced by a factor close to two over all other inelastic channels if isospin is conserved.

The purpose of the present Letter is to supply an experimental test of the prediction of Ref. 4) through a careful analysis of the reaction  $^{11}\text{B}(p,n)^{11}\text{C}$  at  $\langle E_p \rangle = 14.3$  MeV. The cross sections of (p,n) energy averaged transitions to the ground, as well as the first three excited states of  $^{11}\text{C}$ , have been measured at the São Paulo Pelletron facilities. A full discussion of the details of these measurements has already been reported<sup>5)</sup>. Also included in the present analysis is the elastic scattering cross section at  $\langle E_p \rangle = 13.0$  MeV measured by Thomson and Watson et al.<sup>6)</sup>.

The analysis was somewhat complicated by the fact that at this incident proton energy the compound nucleus

formation is accompanied by direct reaction processes.

In such cases one has, in principle, to deal with the problem of several directly coupled channels (the elastic and the different neutron channels) competing with the compound nucleus formation in the distribution of the incoming proton flux. Owing to the inherent complexity of such a calculation, we have opted for a midway solution in which each neutron channel is considered coupled explicitly to the proton channel and not to the other neutron channels. Thus we have effectively replaced the N coupled channels problem by a N-1 two coupled channels problem (the proton channel appears always coupled to one individual neutron channel).

Let us now concentrate on one such pair of coupled channels which we denote by 1 and 2. If we call their respective wave functions  $\psi_1$  and  $\psi_2$ , then the equations that have to be solved are, schematically

$$(E_1 - H_1^0)\psi_1 = V_{12}\psi_2 \quad (1)$$

$$(E_2 - H_2^0)\psi_2 = V_{21}\psi_1 \quad (2)$$

where  $H_1^0$  and  $H_2^0$  are non-hermitian channel Hamiltonians. Their non-hermiticity stems from the fact that we allow compound nucleus formation to occur both in channel 1 and 2.

The exact transition amplitude for the process  $1 \rightarrow 2$  is then

$$T_{1 \rightarrow 2} = \langle \phi_2^{(-)} | V_{21} | \psi_1^{(+)} \rangle \quad (3)$$

where  $\psi_1^{(+)}$  is the exact solution of equation (1), whereas  $\phi_2^{(-)}$  is the solution of (2) with its right-hand side set equal to zero.

Clearly, the complex optical potential which is used to generate  $\psi_1^{(+)}$ , in a reduced effective one-channel problem, must be the one that describes exactly the elastic scattering in channel 1. In contrast,  $\phi_2^{(-)}$  is generated from an optical potential (in a rigorously two-coupled channels situation) which simply generates the correct transmission coefficients in channel 2 that would appear in the Hauser-Feshbach compound nucleus cross section.

Obeying strictly the above criteria, the evaluation of  $T_{1 \rightarrow 2}$  Eq. (3) with a usual DWBA code would generate a transition amplitude, very close to the exact one obtained from the numerical solution of Eqs. (1) and (2). We adhere to the above recipe in our analysis below, always allowing small variations owing to the obvious influence of the other not-explicitly-considered channels. In what follows, channel 1 represents the proton channel and 2 any given neutron channel.

For describing the direct reaction processes we used the computer code DWBA70<sup>7)</sup>. The Bertsch et al.<sup>8)</sup> G-matrix interaction provided the central terms, combinations of spin-isospin scalar and vector interactions, plus the non-central spin orbit and tensor terms whose strengths and ranges were

chosen in accordance with reference 9. Knockout exchange amplitudes were included in the calculations.

In both the incident and emergent channels the distorted waves were obtained using Woods-Saxon complex volume potential which was tailored to follow the Yamaguchi<sup>10)</sup> microscopic interaction interpolated for the  $p + {}^{40}\text{Ca}$  system at  $E_p = 14$  MeV. Electron scattering densities<sup>11)</sup> of  ${}^{11}\text{B}$  and  ${}^{40}\text{Ca}$  were utilized to obtain initial values of the  $p + {}^{11}\text{B}$  geometric parameters. Further adjustment of these parameters was allowed in order to obtain a best optical model fit to the elastic cross section (computer code CRAPONE<sup>12)</sup> which also included a spin orbit interaction. Volume integrals of  $V_R(r)$  are about 20% larger than those of Yamaguchi<sup>10)</sup>. Final values of the geometric parameters were obtained by maximizing the structure (peak to valley ratios) in the calculated ground state neutron direct reaction cross section. Once determined, all potential strengths and geometrical parameters, with the exception of the absorption strength  $W_0$ , were fixed for the entire analysis and for all the (p,n) channels. The variations allowed in  $W_0$  throughout the analysis are discussed in detail below.

The neutron-proton  $Z^J$  coefficients (spectroscopic factors) for these p-shell nuclei involved in the calculation, based on the Lee-Kurath<sup>13)</sup> values, were provided by F. Petrovich and A. Carpenter<sup>14)</sup>. Normalization factors (table 1) for the  ${}^{11}\text{B}(p,n){}^{11}\text{C}$  cross sections resulting from the analysis of Grimes

et al.<sup>15)</sup> at  $E_p = 26$  MeV were applied to all our calculated neutron cross sections.

The Hauser-Feshbach calculation was performed using the code HAUSER-5<sup>16)</sup>. Five modes of decay  $n$ ,  $p$ ,  $d$ ,  $\alpha$  and  ${}^3\text{He}$  were included with a totality of 59 exit channels. Final state continuum channels were deemed unnecessary<sup>17)</sup>.

For the proton and neutron channels the "microscopic" Woods-Saxon optical potential was used to calculate the transmission coefficients. The real potential strength and the geometrical parameters for both the real and imaginary potentials were obtained as described above.

The values of the imaginary part of the optical potential  $W_0^{\text{HF}}$  used in the Hauser Feshbach calculation were obtained from a goodness of fit procedure of the following type. Various Hauser Feshbach distributions were assumed for the  $n_0$  neutrons between zero and an arbitrary upper limit estimated from the  $(p, n_0)$  differential cross section. We denote any given one of these by  $\sigma^{\text{HF}(i)}$ . For simplicity, we considered  $W_0^{\text{HF}}$  (proton) equal to  $W_0^{\text{HF}}$  (neutron) and calculated the value needed to reproduce the  $\sigma^{\text{HF}(i)}$  cross section, labelling it  $W_0^{\text{HF}(i)}$  (proton).

Subtraction of  $\sigma^{\text{HF}(i)}(p, p_0)$  from the experimental elastic cross section gave the shape elastic part of the  $(p, p_0)$  channel,  $\sigma_{\text{se}}(p, p_0)$ . Optical model fits<sup>12)</sup> to this  $\sigma_{\text{se}}(p, p_0)$  determined the value of  $W_0$  (proton) which was subsequently used in the DWBA calculations<sup>7)</sup> for all the  $(p, n)$  channels and referred to as  $W_0^{\text{DWBA}(i)}$  (proton). (Notice that  $\sigma^{\text{HF}(i)}(p, p_0)$  contains the usual width fluctuation factor.)

The value of  $W_0$  (neutron) used in the DWBA in accordance with the discussion following Eq. (3) was assumed to be just the  $W^{\text{HF}(i)}$  (neutron) described above and henceforth called  $W^{\text{DWBA}(i)}$  (neutron). With these values of the absorption potential for the direct reaction process, a DWBA70 calculation was made called  $\sigma^{\text{DWBA}(i)}$ .

The theoretical cross sections for the  $n_1, n_2$  and  $n_3$  neutron groups were obtained from

$$\sigma^{\text{THEOR}(i)}(n_x) = \sigma^{\text{HF}(i)}(n_x) + \sigma^{\text{DWBA}(i)}(n_x) \quad x=1,2,3 \quad (4)$$

and for the ground state neutrons

$$\sigma^{\text{THEOR}(i)}(n_0) = F \sigma^{\text{HF}(i)}(n_0) + \sigma^{\text{DWBA}(i)}(n_0) \quad (5)$$

where  $F$  is the HWR factor<sup>4)</sup>.

This procedure was repeated for eight presupposed HF angular distributions with the goodness of fit to the  $n_1, n_2$  and  $n_3$  experimental cross sections as guide for selecting the most appropriate  $i$ -th-predictions. Once chosen, the HWR factor was tested for goodness of fit to the  $n_0$  differential cross sections. The results, for  $F=2$ , are the full curves shown in Figures 1 and 2. The full dots in these figures are the experimental cross sections with the bars representing their uncertainties and the dashed curve in the  $(p, n_0)$  channel, Figure 1, is the differential cross section for  $F=1$ . The Hauser-Feshbach predictions assumed for the  $n_1, n_2$  and  $n_3$  channels corresponded to a cross section at  $\theta_{\text{CM}} = 90^\circ$  of 0.18 mb/sr, 0.40 mb/sr and 0.32 mb/sr respectively and in the  $n_0$  case 0.40 mb/sr for  $F=1$ .

We conclude that an elastic enhancement,  $F$ , larger than 1 is appropriate for this reaction, which seems to indicate weak isospin mixing in the compound nucleus  $^{12}\text{C}$  at the excitation energy of 29 MeV involved in this work. It would be interesting to further apply our reduced coupled channels model at smaller proton energies, where one expects a larger compound contribution to the cross section, thus increasing the sensitivity with respect to  $F$ . An especially interesting region would be the d-shell nuclei where spectroscopic factors have recently become available<sup>19)</sup> thus permitting a precise description of the direct process with the consequent assessment, through our procedure, of the degree of isospin mixing in this mass region.

ACKNOWLEDGEMENTS

Two of the authors (EFP and HRS) would like to express their deep appreciation to F. Petrovich and A. Carpenter for providing the  $Z^J$  coefficients for p-shell nuclei and preprints of their analysis of  $^{11}\text{B}(p,n)^{11}\text{C}$  at 26 MeV.

We would also like to acknowledge the financial aid extended to us by the Conselho Nacional de Pesquisas (Brazil) and FINEP.

REFERENCES

- 1) M. Kawai, A.K. Kerman, and K.W. McVoy, *Ann. Phys. (NY)* 75, 156 (1973).
- 2) C. Mahaux and H.A. Weidenmüller, *Ann. Rev. Nucl. Part. Sci.* 29, 1 (1979).
- 3) W. Kretschmer and M. Wangler, *Phys. Rev. Lett.* 41, 224 (1978).
- 4) H.L. Harney, H.A. Weidenmüller, and A. Richter, *Phys. Lett.* 96B, 227 (1980).
- 5) H.R. Schelin, E. Farrelly Pessoa, W.R. Wylie, J.L. Cardoso Jr., and R.A. Douglas, *Nucl. Sci. Eng.* 89, 87 (1985).
- 6) W. Thompson, Thesis, Yale (1972), unpublished; B.A. Watson, P.P. Singh, and R.E. Segel, *Phys. Rev.* 182, 977 (1969).
- 7) R. Schaeffer and J. Raynal, computer code DWBA70, updated by W.G. Love, unpublished.
- 8) G. Bertsch, J. Borysowicz, H. McManus, and W.G. Love, *Nucl. Phys.* A284, 399 (1977).
- 9) F. Petrovich, R.H. Howell, C.H. Poppe, S.M. Austin, and G.M. Crawley, *Nucl. Phys.* A383, 355 (1982).
- 10) N. Yamaguchi, S. Nagata, and T. Matsuda, *Prog. Theor. Phys.* 70, 459 (1983).
- 11) C.W. De Jager, H. De Vries, and C. De Vries, *Atomic Data and Nuclear Data Tables*, 14, 479 (1974).
- 12) F. Fabbri and G. Reffo, computer code CRAPONE (1977), unpublished.

- 13) T.S.H. Lee and D. Kurath, Phys. Rev. C21, 293 (1980).
- 14) F. Petrovich and A. Carpenter (private communication).
- 15) S.M. Grimes, J.D. Anderson, J.C. Davis, R.H. Howell, C. Wong, A.W. Carpenter, J.A. Carr, and F. Petrovich, private communication, to be published.
- 16) F.M. Mann, computer code HAUSER-5 (1978), unpublished.
- 17) For the d,  $\alpha$  and  $^3\text{He}$  exit channel the optical potential used was a volume real and surface imaginary whose parametrization were taken from C.M. Perey and F.G. Perey, Atomic Data and Nuclear Data Tables 17, 1 (1976).
- 18) H.R. Schelin, Doctoral Thesis (São Paulo), in preparation; H.R. Schelin, E. Farrelly Pessoa, M.S. Hussein, and R.A. Douglas, to be published.
- 19) B.H. Wildenthal (private communication).

TABLE CAPTIONS

Table 1 - Normalization coefficients applied to the (p,n) cross sections taken from reference 15.

Table 2 - Optical potential strengths (MeV) and geometric parameters (fm) obtained in the analysis for the  $\sigma_{\text{HF}(i)}$  contribution.

FIGURE CAPTIONS

Figure 1 - The elastic differential cross section at  $\langle E_p \rangle = 13.0$  MeV and the ground state charge exchange differential cross section at  $\langle E_p \rangle = 14.3$  MeV for  $^{11}\text{B}+p$ . The full and dashed curves are the theoretical calculations (see text for details).

Figure 2 - The first three excited state differential cross sections at  $\langle E_p \rangle = 14.3$  MeV for  $^{11}\text{B}(p,n)^{11}\text{C}$ . The full curves are the theoretical calculations (see text for details).

TABLE 1

Transition	J	$N_{pn}$ b)	$N_\tau$ c)	$N_{\sigma\tau}$ d)	$N_{TOT}$ e)
$\frac{3}{2}^- \rightarrow \frac{3}{2}^-$ (g.s.)	0	-	0.950	-	0.950
	1	0.618	-	0.640	0.396
	2 <sup>a)</sup>	-	0.950	-	0.475
$\frac{3}{2}^- \rightarrow \frac{1}{2}^-$	3	0.618	-	0.640	0.396
	1	0.330	-	0.640	0.211
	2 <sup>a)</sup>	-	-	0.950	0.475
$\frac{3}{2}^- + \frac{5}{2}^-$	1	0.970	-	0.640	0.621
	2 <sup>a)</sup>	-	0.950	-	0.475
	3	0.970	-	0.640	0.621
$\frac{3}{2}^- + \frac{3}{2}^-$ (e.s.)	1	0.470	-	0.640	0.301
	2 <sup>a)</sup>	-	0.950	-	0.475
	3	0.470	-	0.640	0.301

a) Reduction factor of 2 (account for the isovector quadrupole renormalization), Ref. 9.

b) Nuclear wave functions normalization, Ref. 15.

c) Isovector interaction  $g_{01}$  normalization, Ref. 9 and 15.

d) Isovector interaction  $g_{11}$  normalization, Ref. 9 and 15.

e)  $N_{TOT} = N_{pn} N_\tau$  or  $(N_{pn} N_{\sigma\tau})$ .



TABLE 2

	$V_R$	$r_R$	$a_R$
proton and neutron	50.00	1.35	0.56
	$W_0^{DWBA}$	$r_w$	$a_w$
proton	7.17	1.63	0.23
neutron	2.47	1.63	0.23
	$W_0^{HF}$	$r_w$	$a_w$
proton and neutron	2.47	1.63	0.23
	$V_{so}$	$r_{so}$	$a_{so}$
proton and neutron	5.10	1.19	0.43

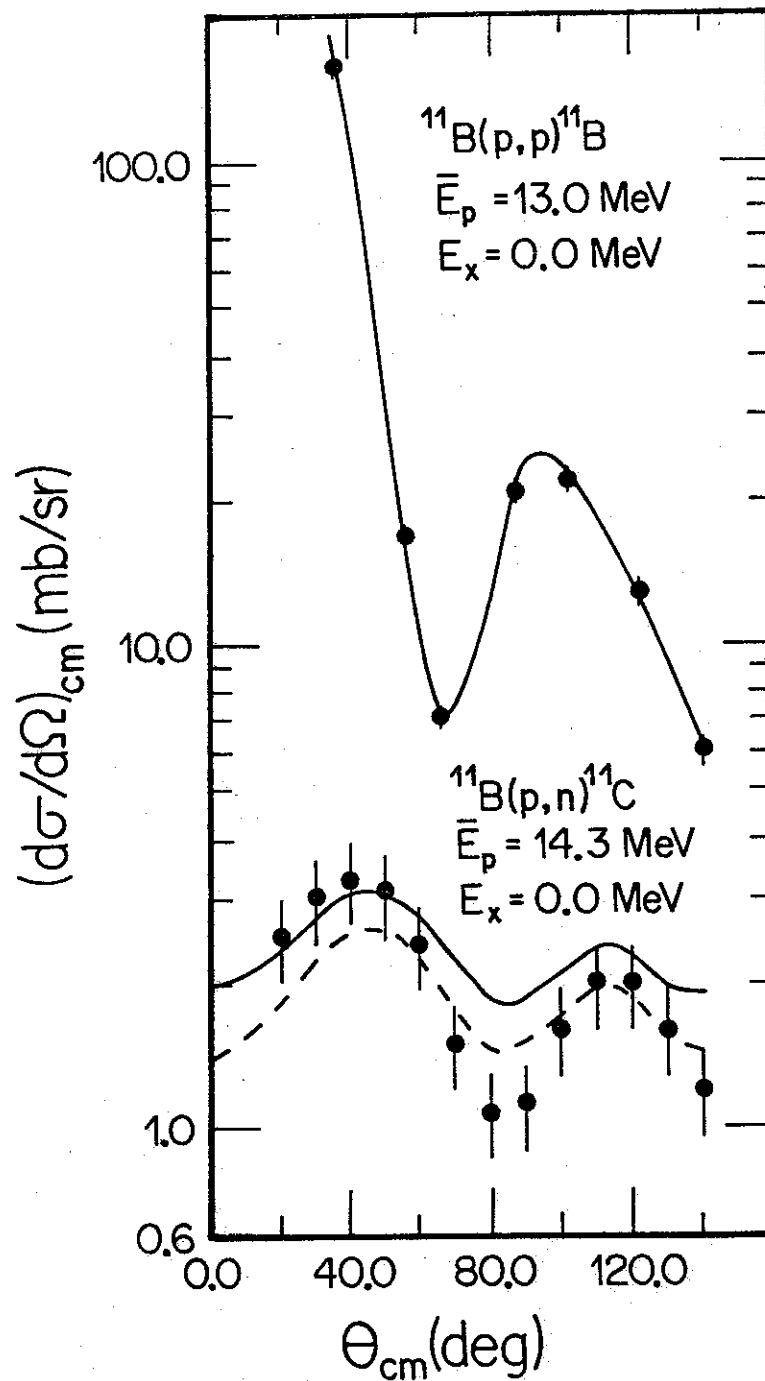


Fig. 1

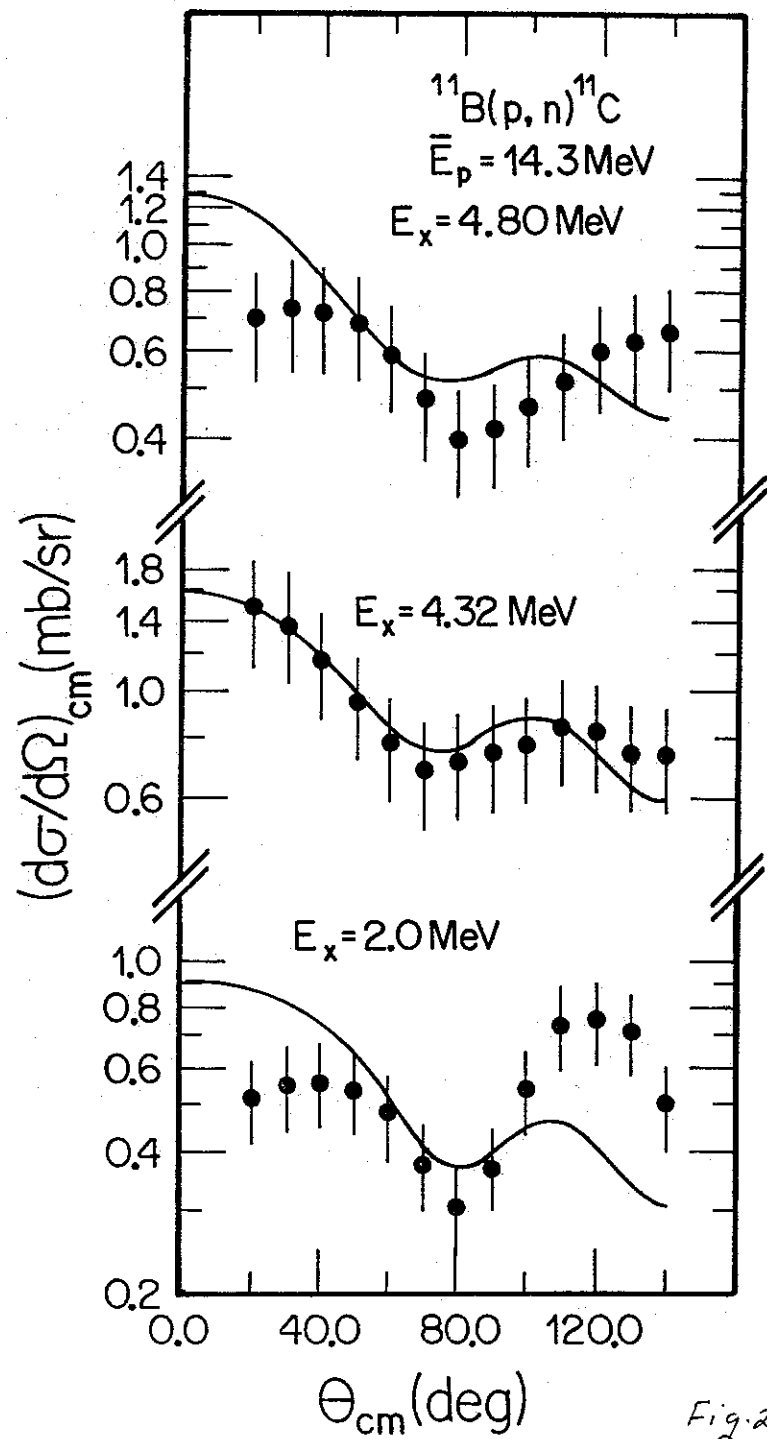


Fig. 2